First measurement of time evolution of electron temperature profiles with Nd:YAG Thomson scattering system on Heliotron J

Kenmochi, N.; Minami, T.; Takahashi, C.; Tei, S.; Mizuuchi, T.; Kobayashi, S.; Nagasaki, K.; ... Ohtani, Y.; Kasajima, K.; Sano, F.

AIP | Review of Scientific Instruments

First measurement of time evolution of electron temperature profiles with Nd:YAG Thomson scattering system on Heliotron Ja)

N. Kenmochi, T. Minami, C. Takahashi, S. Tei, T. Mizuuchi, S. Kobayashi, K. Nagasaki, Y. Nakamura, H. Okada, S. Kado, S. Yamamoto, S. Ohshima, S. Konoshima, N. Shi, L. Zang, Y. Ohtani, K. Kasajima, and F. Sano

Citation: Review of Scientific Instruments **85**, 11D819 (2014); doi: 10.1063/1.4890255
View online: http://dx.doi.org/10.1063/1.4890255
View Table of Contents: http://scitation.aip.org/content/aip/journal/rsi/85/11?ver=pdfcov
Published by the AIP Publishing

REVIEW OF SCIENTIFIC INSTRUMENTS **85**, 11D819 (2014)

First measurement of time evolution of electron temperature profiles with Nd:YAG Thomson scattering system on Heliotron J[a)]

N. Kenmochi,[1,b)] T. Minami,[2] C. Takahashi,[2] S. Tei,[1] T. Mizuuchi,[2] S. Kobayashi,[2] K. Nagasaki,[2] Y. Nakamura,[2] H. Okada,[2] S. Kado,[2] S. Yamamoto,[2] S. Ohshima,[2] S. Konoshima,[2] N. Shi,[2] L. Zang,[1] Y. Ohtani,[1] K. Kasajima,[1] and F. Sano[2]
[1]*Graduate School of Energy Science, Kyoto University, Gokasho, Uji 611-0011, Japan*
[2]*Institute of Advanced Energy, Kyoto University, Gokasho, Uji 611-0011, Japan*

(Presented 3 June 2014; received 1 June 2014; accepted 2 July 2014; published online 22 July 2014)

A Nd:YAG Thomson scattering system has been developed for Heliotron J. The system consists of two 550 mJ 50 Hz lasers, large collection optics, and 25 radial channel (∼1 cm spatial resolution) interference polychromators. This measurement system achieves a S/N ratio of ∼50 for low-density plasma ($n_e \sim 0.5 \times 10^{19}$ m^{-3}). A time evolution of electron temperature profiles was measured with this system for a high-intensity gas-puff (HIGP) fueling neutral-beam-injection plasma. The peripheral temperature of the higher-density phase after HIGP recovers to the low-density pre-HIGP level, suggesting that improving particle transport in the HIGP plasma may be possible. © *2014 AIP Publishing LLC*. [http://dx.doi.org/10.1063/1.4890255]

I. INTRODUCTION

A high temporal and spatial resolution Nd:YAG laser Thomson scattering (TS) system for Heliotron J ($L/M = 1/4$, $\langle R_0\rangle/\langle a_0\rangle = 1.2$ m/0.17 m, $\langle B_0\rangle \leqq 1.5$ T) has been developed for detailed study of the time evolution of electron temperature (T_e) and density (n_e) profiles. In Heliotron J, spontaneous transition to an improved confinement mode has been observed.[1] In addition, Heliotron J achieves high-density and high-performance plasmas with high-intensity gas-puff (HIGP) fueling[2] and supersonic molecular beam injection.[3] These two fueling techniques have been applied not only to control the core plasma density but also to modify the edge plasma density. Since the profile changes of T_e and n_e are important in these phenomena, the TS system provides indispensable information for realization of good performance plasmas.

This article provides an overview of the diagnostic system; moreover, it describes the details of the polychromator system and reports the first measurement of the time evolution of T_e profile in a high-density neutral-beam-injection (NBI) plasma implemented by HIGP.

II. DESCRIPTION OF THE SYSTEM

The Heliotron J TS system consists of two 550 mJ 50 Hz Nd:YAG lasers with a pulse width of 10 ns, a beam dump, large collection optics, and 25 radial channel (∼1 cm spatial resolution) interference polychromators. Figure 1 shows a schematic side view of the TS system on Heliotron J. To reduce stray light from reflections at the input and output vacuum windows of Heliotron J, the laser beams approach and leave Heliotron J through long evacuated pipes. In addition, the laser beams are introduced into the plasma at an oblique angle (from a low point outside the torus to a higher point inside the torus). A carbon beam dump installed downstream of the output window absorbs the laser beams. The obliquely backscattered light is reflected by a large concave mirror (D = 820 mm, f/1.25) with a solid angle of 45 to 55 × 10^{-3} str to the entrance of a staircase-form fiber bundle, which guides the light to 25 polychromators. This configuration has an improved signal-to-noise (S/N) ratio, which is due to the small background plasma region accepted by the collection optics. The fibers are polymer-clad optical fibers made by Mitsubishi Cable Industries, Ltd. (3 mm × 1.5 mm, NA = 0.39, 12 core wires). We developed a new laser timing controller to precisely control the injection timing of the laser pulses with respect to plasma discharge.[4] The designed target plasma range is 10 eV $< T_e <$ 10 keV and $n_e > 0.5 \times 10^{19}$ m^{-3}.

III. POLYCHROMATOR

Spectral analysis of the scattered light was performed by interference-type polychromators, similar to those used in DIII-D.[5] Each polychromator consists of interference filters, a relay lens, avalanche photodiodes (APD; Hamamatsu photonics K.K., S 8890-30), and fast-response preamplifiers. The scattered light is cascaded between five interference filters by using relay lenses and divided into five spectral channels. The light from each channel is then focused onto an APD, where it is converted to an electrical signal. The spectral band ranges of the five channels are selected according to the expected electron temperature range (0.1–10 keV) of Heliotron J.[6] One spectral channel has no filter and is used for calibration by Rayleigh scattering.

The preamplifier for each APD has two outputs: a directly coupled channel to measure the background light and a high-pass channel, which reduces the background light by using a RC filter, to measure the scattered laser pulses.

[a)]Contributed paper, published as part of the Proceedings of the 20th Topical Conference on High-Temperature Plasma Diagnostics, Atlanta, Georgia, USA, June 2014.

[b)]Author to whom correspondence should be addressed. Electronic mail: kemmchi.naoki.62r@st.kyoto-u.ac.jp

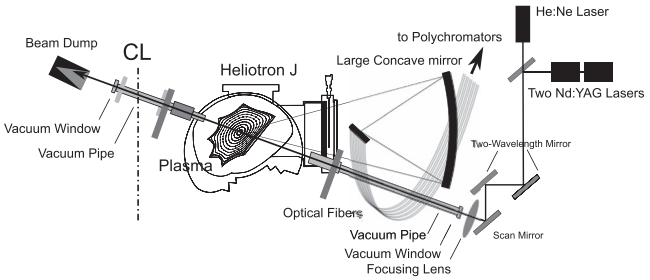

FIG. 1. Schematic of Nd:YAG laser Thomson scattering system for Heliotron J.

A. Effect of temperature on APD sensitivity

Since APD sensitivity depends on its temperature, we compensate temperature-induced changes in the sensitivity by feedback control of the bias voltage from a regulator (Matsusada Precision Inc. HAPD-0.8PT) based on the temperature monitor attached to the APD. We verified the proper functioning of this compensator by performing two experiments.

In the first experiment, which was performed at room temperature (25 °C), the change in APD sensitivity was monitored for three hours after the power supply was turned on. Light produced by a light-emitting diode system was introduced by an optical fiber into the polychromators to provide a constant illumination. Figure 2(a) shows the time trace of APD sensitivity. With (without) the temperature compensator, the sensitivity stabilizes within 0.5 (1.5) h. The rapid stabilization with the temperature compensator indicates that the system may be used relatively quickly after it is powered on.

We also measured the shift in APD sensitivity due to changing room temperature from 17 °C to 34 °C. Figure 2(b) shows the time traces of the APD output and the associated room temperature. This experiment was performed 2 h after the APD power supply was turned on. The APD output

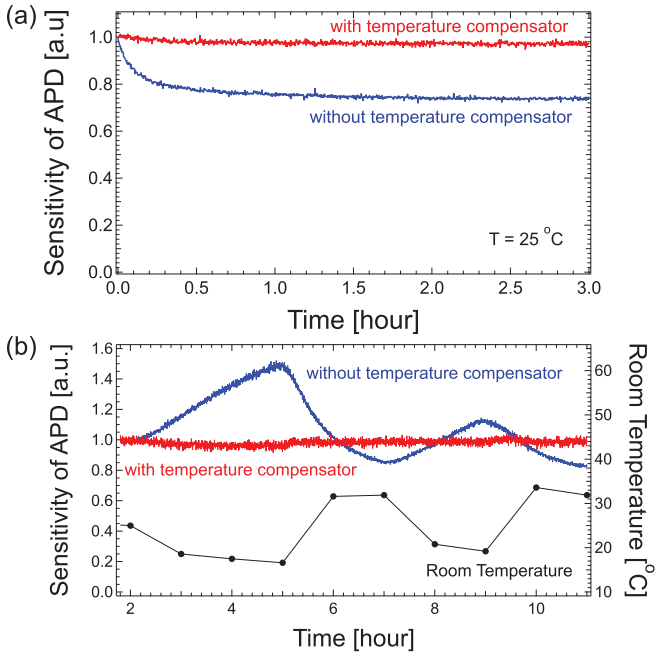

FIG. 2. APD outputs at (a) constant room temperature (25 °C) and (b) varying room temperature (17 °C to 34 °C).

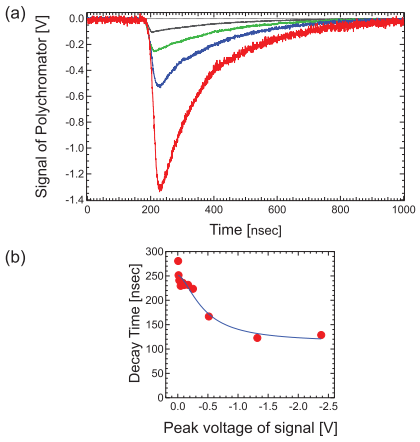

FIG. 3. (a) Temporal response of APD to various input power. (b) Decay time of APD as a function of input power.

varied by ∼4.1%/°C without the compensator and only 0.31%/°C with the compensator. These results show that the system provides accurate measurements of T_e and n_e despite variations in the surrounding temperature.

B. APD response speed

Precise measurements require a linear APD sensitivity for a pulsed input. The linearity for steady-state illumination was confirmed in our previous calibration study; here, we investigate the APD response to pulsed light. To do this, we illuminated an APD with Nd:YAG laser pulses and varied the illumination power with laser attenuators. The results are shown in Fig. 3(a). The decay time of the low-intensity signal is longer than that of the high-intensity signal. We also evaluated the decay times from the output signals by fitting the dynamics to an exponential decay, $\exp(-t/\tau)$, where τ is the decay time constant. The results for τ are shown in Fig. 3(b). The decay times increase as the peak voltages decrease. To ensure an APD response that is linear in illumination power, we set the gate length for data acquisition as ∼400 ns from t = 150 ns to 550 ns. Since a longer gate decreases the signal-to-noise (S/N) ratio, this adjustment represents a trade-off between APD linearity and S/N.

IV. RESULTS OF INITIAL MEASUREMENTS

A. Test of the measurement system performance

To confirm the S/N ratio of the system for low-density and weakly scattering plasmas, we measured TS signals for the density of ∼0.5 × 10^{19} m^{-3}. Figure 4 shows the raw data of scattered light for the wavelength range 1050–1060 nm, which is close to the wavelength of the Nd:YAG laser (1064 nm). The clear signal is synchronized with the laser pulse. The sources of noise for the system are mainly stray light, background light, and thermal noise from the APD circuit. The background light is reduced by a RC filter. The thermal noise is suppressed during the data-acquisition integration process. The signal without plasma discharge is also shown in Fig. 4. Although the laser beam is injected into the vacuum vessel, no significant changes are observed.

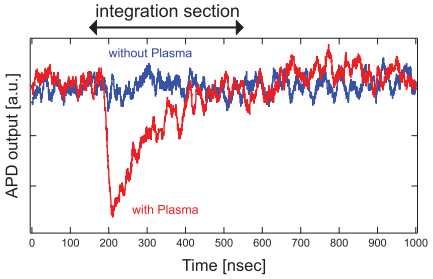

FIG. 4. Raw data of scattered light emitted from a polychromator.

Consequently, we conclude that the system suppresses stray light. The ratio between the scattered light and noise is calculated by integrating each signal over 400 ns. The S/N ratio exceeds 50, which indicates that the system design allows us to collect adequate scattered light.

B. Time evolution measurement of T_e profiles of high-performance plasma

The time evolution measurement of the electron temperature is demonstrated. Figure 5(a) shows the time evolution of the line-averaged density $\overline{n}_e$ and the stored energy W_p in the HIGP plasma. The plasma is initiated by short-pulse electron-cyclotron heating and is sustained only by co-NBI with a port-through power of 0.46 MW. The working gas is deuterium. The HIGP is applied from $t = 220$ to 230 ms, where the D_2 gas is fueled at a fueling rate several times higher than that for the normal gas and with a short period (10 ms). Just after the HIGP, $\overline{n}_e$ increases rapidly and W_p degrades slightly. Next, W_p continues to rise in spite of no gas puffing. The radial T_e profiles of the plasma were measured with the TS system every 5 ms during plasma discharge with 5 ms shifts in the measurement timings for the plasmas whose parameters were reproducible. Profiles for three characteristic timings are shown in Fig. 5(b): just before ($t = 220$ ms), just after ($t = 230$ ms), and 20 ms after ($t = 250$ ms) the HIGP. The T_e characteristics in the peripheral region differ from those in the core region. Figure 5(c) shows the time traces of T_e normalized by T_e at $t = 220$ ms for two positions: the core ($r/a \sim 0$) and the periphery ($r/a \sim 0.9$). From $t = 220$ to 230 ms, T_e decreases, especially in the peripheral region, which indicates that the plasma shrinks. Immediately after that, the peripheral T_e starts to increase, whereas the core T_e continues decreasing. From ~5 ms before the maximum W_p ($t = \sim 250$ ms), the core T_e starts increasing and the peripheral T_e is slightly higher than that before the HIGP ($t = 220$ ms). These results indicate that the peripheral T_e recovers more quickly and completely than the core T_e. Because of the increase in W_p, n_e increases after the HIGP. In spite of the increase of ne, the peripheral T_e recovers to a temperature above the pre-HIGP temperature. This experiment suggests that the particle transport is improved in the HIGP plasma.

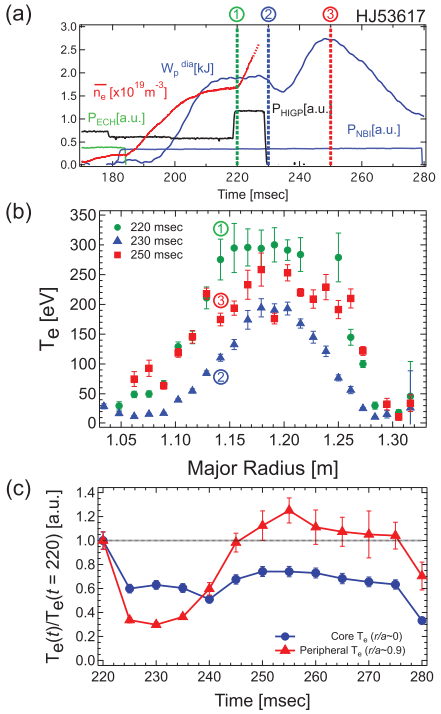

FIG. 5. (a) Time traces of line-averaged density, stored energy in plasma, and timings of ECH, NBI, and HIGP. (b) Time evolution of T_e profiles for NBI-sustained plasma at 230, 240, and 250 ms. (c) Time traces of T_e normalized by T_e at $t = 220$ ms.

V. SUMMARY

We developed a TS system for Heliotron J to measure the time evolution of T_e and n_e profiles with high spatial and temporal resolution. The Heliotron J TS system consists of two 550 mJ 50 Hz Nd:YAG lasers with a pulse width of 10 ns, a beam dump, large collection optics, and 25 radial channel (~1 cm spatial resolution) interference polychromators. The APDs are equipped with temperature compensators to minimize variations in APD sensitivity due to thermal fluctuations. Because the decay time of the APD becomes significant for low input power from the pulsed laser, we use a long gate length for data acquisition to ensure satisfactory linearity in the APD response. This measurement system achieves a S/N ratio of ~50 for a low-density plasma ($n_e \sim 0.5 \times 10^{19}$ m^{-3}). With this system, we measured the time evolution of T_e profiles for a high-density plasma with HIGP fueling. The time evolution of T_e profiles reveal that the peripheral T_e increases after the HIGP and suggests that particle transport in HIGP plasmas may be improved.

ACKNOWLEDGMENTS

This work was supported by the Collaboration Program of the Laboratory for Complex Energy Process, Institute of Advanced Energy, Kyoto University, and the NIFS Collaborative Research Program (NIFS10KUHK030, NIFS09KUHL, and NIFS10KUHL033).

[1]F. Sano *et al.*, Nucl. Fusion **45**, 1557 (2005).
[2]T. Mizuuchi, F. Sano *et al.*, IAEA-FEC2012, 8–13 October 2012, San Diego, USA, EX/P3-07.
[3]T. Mizuuchi *et al.*, J. Nucl. Mater. **415**, S443–S446 (2011).
[4]N. Kenmochi *et al.*, Plasma Fusion Res. **8**, 2402117 (2013).
[5]T. N. Carlstrom *et al.*, Rev. Sci. Instrum. **61**, 2858 (1990).
[6]T. Minami, S. Kobayashi, T. Mizuuchi, H. Yashiro, M. Takeuchi, S. Ohshima *et al.*, Rev. Sci. Instrum. **81**, 10D532 (2010).